International Journal of Microwave and Wireless Technologies

cambridge.org/mrf

Light controlled frequency reconfigurable antenna for wireless applications

V. Reji and C. T. Manimegalai

ECE Department, SRM Institute of Science and Technology, Chennai, India

Abstract

In this paper, a light-controlled frequency reconfigurable antenna is presented for 5 G, WLAN, and radio altimeter applications. The given (44×28) mm^2 antenna consists of a radiating V-shaped structure and three stub arrangements. The main $\lambda/2$ length stub is used to feed the antenna and the two $\lambda/4$, $\lambda/8$ length open-circuited stubs are located perpendicular to the main feeding stub for tuning the frequency of the antenna. The length of the stubs can be adjusted by placing (4×1.2) mm photodiode switches on the perpendicular stubs. Four experiments are carried out to analyze the performance of the antenna. When light and DC bias voltage is not applied (Experiment-1) to the photodiodes the proposed antenna radiates from 4.1 to 4.63 GHz with 12% bandwidth. When light is applied to the photodiode without DC bias voltage and DC bias voltage is applied without light (Experiment-2,3) the antenna reconfigures its frequency band from 3.43 to 3.6GHz and 4.8 to 5.4 GHz with 4.85% and 12% bandwidth respectively. The antenna shifts the radiation from 4.8 to 5.5 GHz with 14% bandwidth when the light and DC bias voltage is applied to the antenna (Experiment-4). The measured gain of the proposed antenna is greater than 3.8dBi in all the experiments.

Research Paper

Cite this article: Reji V, Manimegalai CT (2023). Light controlled frequency reconfigurable antenna for wireless applications. *International Journal of Microwave and Wireless Technologies* **15**, 143–149. https://doi.org/10.1017/S1759078722000137

Received: 10 September 2021
Revised: 15 January 2022
Accepted: 17 January 2022
First published online: 16 February 2022

Keywords:
Light; switch; diode; stub; experiment; bias

Author for correspondence:
C.T. Manimegalai,
E-mail: manimegc@srmist.edu.in

Introduction

The optically controlled reconfiguration technology is a combined technology of optical and electrical fields because it reconfigures the characteristics of the antennas and the operating bands of the filter circuits through switches. The new trend of wireless optical technology is smart lighting and the internet of things. In this technology, multiple electronic devices and smart LED bulbs can be controlled through a common cloud. The ON and OFF state of the LED bulbs are utilized to change the frequency and radiation pattern of the antenna. If these antennas are connected to the electronic devices that can be in contact with some other wireless frequency applications by the smart control of the LED bulbs without connecting any additional devices.

The most common multiband and frequency reconfiguration techniques with PIN and varactor diode switches and lumped elements have been presented in [1–4]. An optical receiving antenna has been developed with a multiband radio frequency transceiver for visible light and optical wireless communications [5, 6]. An antenna was introduced with a low power optical switch for X-band applications [7]. In this antenna, optically controlled SPDT switches are used to route the RF signal into the antenna. A stub loaded frequency reconfigurable antenna has been developed with photoconductive switches [8]. The total frequency shift achieved by this antenna is 0.3GHz. Two 0.3mm thickness silicon switches were controlled by an 850 nm optical signal to reconfigure the frequency from 28 to 38 GHz in [9] and their modulation scheme was discussed in [10]. An optically controlled phased array antenna system with true-time delay devices [11] and an optically feeding array antenna has been developed with high power photodiodes for frequency reconfiguration [12]. Next a slotted circular waveguide antenna at 5.8 GHz with 10% bandwidth and an E-shaped patch antenna at 2.4 and 5.8 GHz with a return loss of −12 dB and −40 dB respectively has been reported for Wi-Fi applications. In both cases, silicon dies and PIN diodes are used as switching elements [13, 14]. More optically controlled antennas have been developed for frequency reconfiguration, Impedance tuning and cognitive radio applications. The operative frequency of the antennas are (2.26 to 3.15 GHz), (100 MHz to 40 GHz) and (3.1 to 10.6 GHz) respectively. All of the above cases used silicon die switches that were activated by a 980nm optical fiber [15–17]. A planner 150×200 mm^2 yagi-uda antenna was demonstrated for pattern reconfiguration with 2 PIN photodiodes. The maximum of 6.3 dbi gain was demonstrated in [18]. An optically controlled antenna is presented with a commercially available photodiode and phototransistors for reconfiguration [19]. The selected wavelength ranges for the above cases are 850 to 1550 nm.

In this paper, a novel optically controlled frequency diversity antenna is proposed for wireless applications. The proposed antenna is a compact, high gain; small dimension and

© The Author(s), 2022. Published by Cambridge University Press in association with the European Microwave Association

CAMBRIDGE UNIVERSITY PRESS

Table 1. Proposed antenna comparison with reference (lit.) antennas

References	No. of Bands (GHz) Switch ON	Switch OFF	Minimum and Maximum Gain (dBi)	Total area (λo)	Count of diodes	Reconfiguration	Applications
[2]	2.89–4.07	5.1–6.19	2.5 2.6	0.66 × 0.66 × 0.021	4-PIN diode	Yes	5G, WLAN
[14]	2.81–3.73,1.94–2.14	3.17–3.91, 2.34–2.94	1.25 2.2	0.37 × 0.37 × 0.016	2-PIN Diodes	Yes	5G, LTE, Wi-Fi, Wi-Max
[17]	2.5	5.2(notch bands)	3	0.53 × 0.66 × 0.02	2-Silicon Dies	Yes	Wi-Max, WLAN
[18]	1.8–2.37	2.1–2.35	5.8	1.10 × 1.47 × 0.011	2-PIN photo diodes	Yes	Wireless applications
Proposed antenna	4.8–5.5	3.43–3.6,4.8–5.4,4.1–4.63	3.8 7.2	0.58 × 0.37 × 0.02	2-Photo diodes	Yes	WLAN, 5G, Radio Altimeter

multiband (4-bands) antenna compared with the reference antennas in Table 1. The photodiode switches were activated by optical fiber cables in the previous works. But in this work, two commercially available photodiodes are used for switching and they are activated by an LED bulb. If these antennas will be connected in aircraft landing systems at 4.3GHz it can reconfigure their frequency to wireless LAN and 5 G applications by the smart control of the LED bulbs without connecting any intermediate devices.

Antenna design techniques

Antenna structure

The proposed antenna is designed on Roger RO3003(tm) substrate with a substrate thickness of $z = 1.52$ mm, the permittivity of $\epsilon_r = 3.3$ and the loss tangent of 0.0013. This antenna is a long wire V antenna model [20]. Two 8mm length and 1.2mm width legs are arranged in the shape of V with one end of the V-shape is connected to the feeding stub and the next end of the wire is left to be opened. The length of the legs is calculated by $\lambda/4 < (2\times l3 + l2) < \lambda/2$ ($f_o = 4$ GHz, $2 \times l3 + l2 = 2 \times 8 + 4 = 20$ mm).

The center frequency of the V-shaped radiator $f_o = 4$GHz and the length of the feeding stub is $\lambda/2$. Two 14.4 mm($\lambda/4$) and 9.5 mm($\lambda/8$) length and 1mm width open-circuited stubs are connected perpendicular with the feeding stub. 4 mm length and 1.2 mm width photodiode switches [20] are placed along with 2 pf blocking capacitors on the perpendicular stubs. The ground area of the substrate is reduced to 32 mm for increasing the gain of the antenna. The antenna structure and their stub arrangement with photodiodes are illustrated in Figs 1(a) and (b).

Calculation of tuning stubs

The antenna design can be explained by a simple transmission line model with a stub tuning method. The stubs are located first at $Y_{IN}/G_o = 1$ position then the location will be adjusted by the equation (1). The lengths of the tuning stubs are calculated by equations (2)–(5). The effective lengths of the stubs are decided only by the conductivity of the photodiode switches. When the photodiodes are in OFF condition the conductivity $G \to 0$, l_{ef1} and $l_{ef2} = 0$, then the value of $l_4 = l_{t1}$ and $l_5 = l_{t2}$. The relationship between l_{t1}, l_{t2} and l_{ef1} and l_{ef2} are given in Fig. 4. When the photodiodes are in ON state the value of G is changed according to equation (2) and it changes the effective length of the stubs. If the antenna stub lengths are changed their resonant frequency is also changed from f_o to some other value. The variations of G is calculated from the input admittance equation $Y_{IN} = G + J\omega c$.

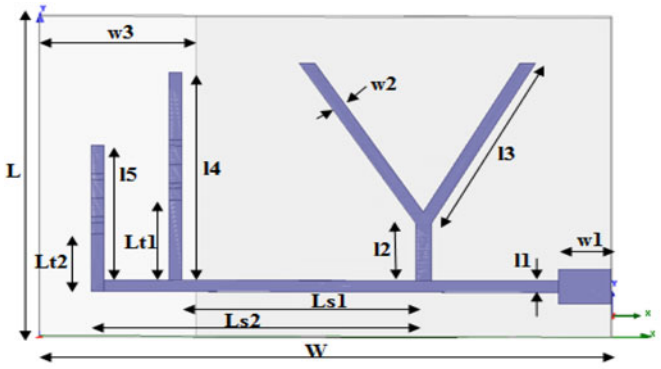
$$Y_r tan^2 \beta L_s = 1 \tag{1}$$

$$\beta l_{ef1} = \tan^{-1} \frac{\sqrt{G}}{1 - G} \tag{2}$$

$$l_4 = L_t 1 + l_{ef1} \tag{3}$$

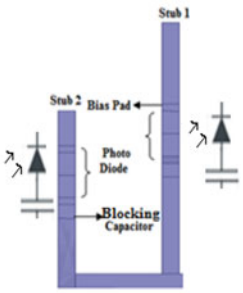
$$\beta l_{ef2} = \tan^{-1} \frac{\sqrt{G}}{1 - G} \tag{4}$$

https://doi.org/10.1017/S1759078722000137 Published online by Cambridge University Press



($W = 44$, $L = 28$, $w1 = 4$, $w2 = 1.2$, $w3 = 12$, $Ls1 = 20$, $Ls2 = 25$, $Lt1 = 7$, $Lt2 = 5$, $l1 = 1.5$, $l2 = 4$, $l3 = 8$, $l4 = 18.15$, $l5 = 12.75$).

(a)



(b)

Fig. 1. (a) Antenna with dimensions in mm (b) Antenna Stub arrangements.

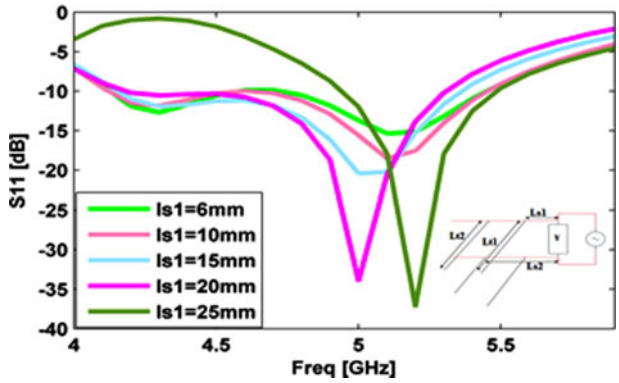


Fig. 2. Location of the stub Ls_1 from V-shaped radiator.

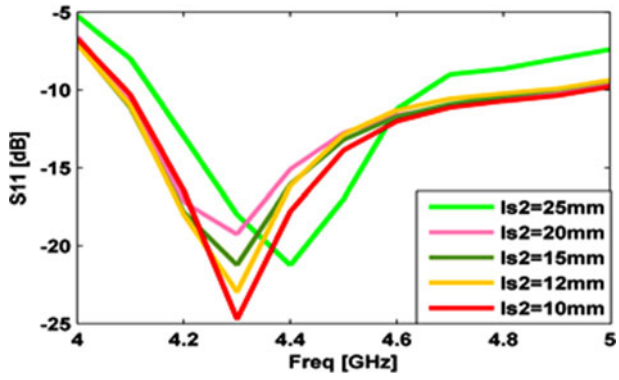


Fig. 3. Location of the stub Ls_2 from V-shaped radiator.

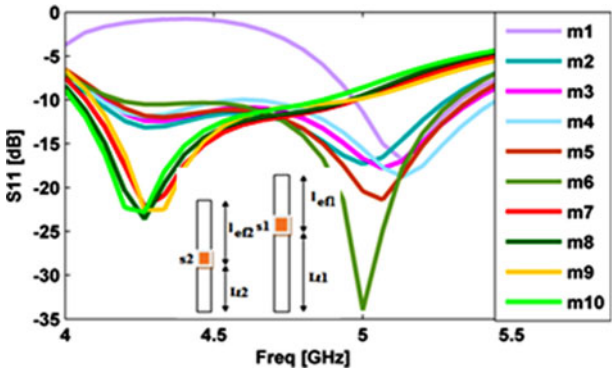


Fig. 4. Position of the switch Lt_1 and Lt_2 in mm ($m1$-2,1.5 $m2$-4,3 $m3$-6,4.5 $m4$-7,5 $m5$-10,7.5 $m6$-12,9 $m7$- 14,10.5 $m8$-16,12 $m9$-18,13.5 $m10$-19,15).

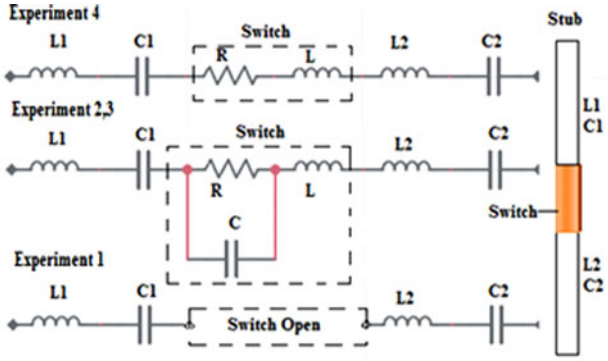


Fig. 5. Equivalent circuit of the switch.

$$l_5 = L_t2 + l_{ef2} \tag{5}$$

$Y_r \rightarrow$ Load Admittance $\beta \rightarrow 2\pi/\lambda$(phase constant)
$G \rightarrow$ Conductance $l_{ef} \rightarrow$ Effective length of the stubs

A Parametric study is done for finding the location of the stubs (ls_1, ls_2) from the load and the position of the switch on the stub (lt_1, lt_2) as illustrated in Figs 2–4. The position of the switch $s1$ is considered from 2 to 18 mm and the position of the switch s_2 is considered from 1.5 to 15 mm from the feeding stub. When the value of $L_{t1} = 7$ mm and $L_{t2} = 5$ mm, the antenna is giving a better solution compared with other solutions. The analysis shows the two best locations to connect the first stub from the V-shaped radiator, that is $Ls_1 = 20$ mm and $Ls_1 = 25$ mm. But for the proposed antenna design 20 mm distance is selected from the V-shaped radiator because the next stub should be connected within $0.25\,\lambda$. The location of the second stub is connected at 25 mm from the V-shaped radiator. At this position, the antenna is radiating at 4.3 and 5 GHz with return loss values of −34.5dB and −30 dB respectively.

https://doi.org/10.1017/S1759078722000137 Published online by Cambridge University Press

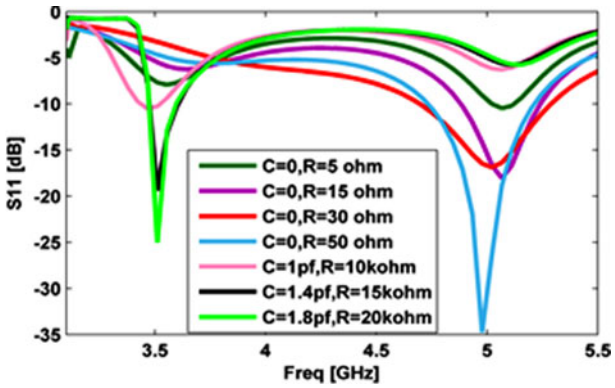


Fig. 6. *R* and *C* values of the Optical Switch.

Switch and bias circuit design

4×1.2 mm length and 0.85 mm thickness photodiodes are selected as a switch for simulation. These switches are activated by a light signal with or without DC bias voltage. The switch is connected serially between the two resonant circuits C1, L1 (upper part of the stub) and C2, L2 (lower part of the stub) as shown in Fig. 5. Experiment-1 is simulated without DC bias and light, Experiment-2, 3 are simulated through the lumped element assignment of photodiodes with the values $R = 20\,\text{k}\Omega$, $C = 1.8$ pf, $L = 1$ nH and $R = 40\,\text{k}\Omega$, $C = 1.8$ pf, $L = 1$ nH. Experiment-4 is simulated by assigning the values $R = 50\,\Omega$ and $L = 1$ nH for the photodiodes. The effective length of the stubs can be adjusted by the internal resistance and capacitance variations of the switch.

$$Y_{IN} = \frac{1}{R} + j\omega c \tag{6}$$

Figure 6 shows the antenna radiation frequencies at different resistance and capacitance values. At $R = 50\,\Omega$ and $L = 1$ nH the antenna is radiating at 5 GHz and the values of $R = 20$ k, $C = 1.8$ pf the antenna is radiating at 3.5 and 5 GHz. But minimum return loss is achieved only at 5 GHz range at −0.5 to −1 DC biasing. This parametric analysis is done with the internal inductance value of 1nH and the blocking capacitance value of

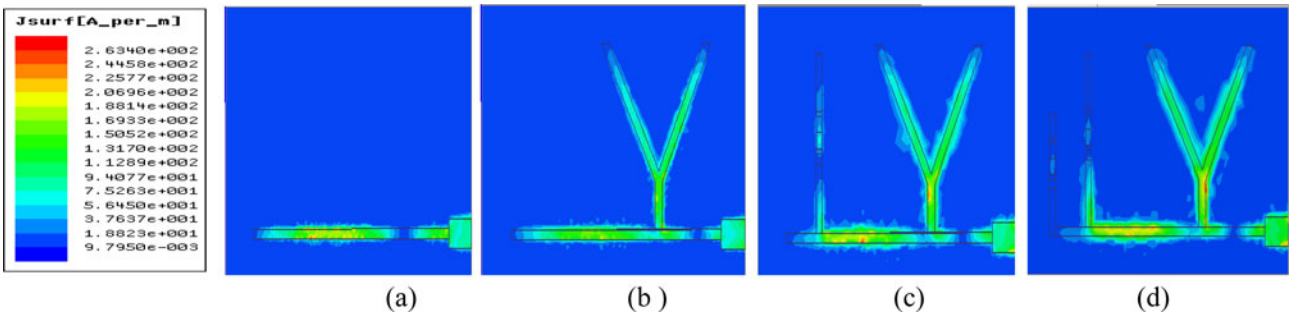


Fig. 7. Surface current distribution with (a) a feeding stub (b) Y-shaped radiator (c) Single stub (d) Double stub.

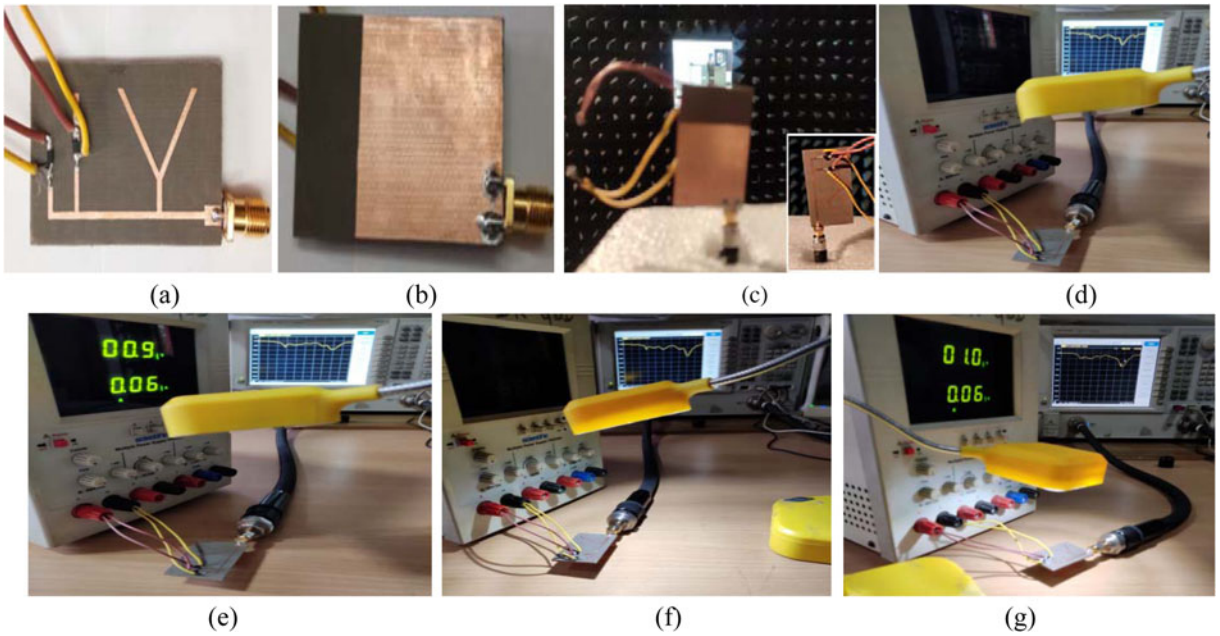


Fig. 8. Fabricated antenna (a) Top view (b) Bottom View (c)Antenna pattern measurement at the anechoic chamber (d) Experiment-1(No DC bias and light) (e) Experiment-2(DC bias without light) (f) Experiment- 3 (Light present without DC bias) (g) Experiment-4 (light with DC bias).

https://doi.org/10.1017/S1759078722000137 Published online by Cambridge University Press

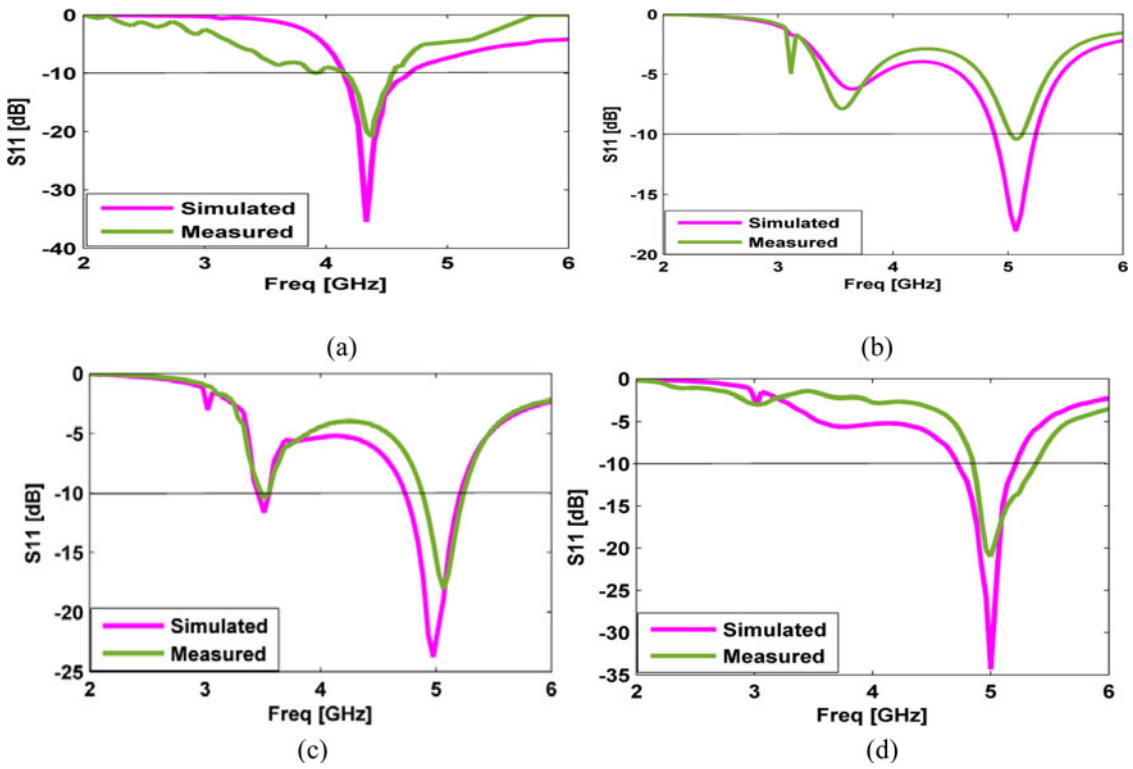


Fig. 9. Simulated and measured antenna S_{11} parameters at (a) Exp.-1 (b) Exp.-2 (c)Exp.-3 (d) Exp.-4.

Table 2. Simulation and measurement results comparison of the proposed antenna.

	Frequency (GHz)		Return Loss(dB)		Gain(dBi)		Efficiency	
Experiments	Simulated	Measured	Simulated	Measured	Simulated	Measured	Simulated	Measured
Experiment-1	4.3	4.32	−35.4	−21	4.2	3.8	0.52	0.4
Experiment-2	3.5 and 5	3.57 and 5	−6.2,-18	−8.3, −10	7	6.3	0.54	0.45
Experiment-3	3.5 and 5	3.5 and 5.1	−11,-24.7	−10.2, −18.5	7	6.3	0.54	0.45
Experiment-4	5	5	−35	−20	8	7.2	0.8	0.72

2pf. The simulation results show the return loss value of −35 dB at 5 GHz.

Current distribution in antenna geometry

Figure 7 shows the current density flow of the antenna geometry. The values are given in blue color indicate low current density and upper values indicate high current density. When the feeding stub is only connected to the antenna their maximum field distribution is toward the end of the feeding stub. The V-shaped radiator is also connected to the feeding stub the electric field is moving toward the legs of the radiator. When the two tuning stubs are connected to the V-shaped radiator through the feeding stub, the field is moving toward the top of the tuning stubs. We can see that the involvement of tuning stubs and effective length of the tuning stubs with their current density flow in Figs 7(c) and 7(d).

Results and discussion

The antenna prototype is fabricated on Roger substrate with the dielectric constant of $\epsilon_r = 3.3$ and the substrate thickness of 1.52 mm as shown in Figs 8(a) and 8(b). Roger substrate is a good choice for fabricating microstrip antennas because it reduces the dielectric loss and increases the gain at high frequencies over Fr-4 substrate. Two 4 mm length and 1.2 mm width TEMD7100IT SMD silicon PIN photodiodes are connected on the stub for switching purposes. The thickness of the switch is 0.85 mm and the radiant sensitive area is 0.23 mm^2. A 5 watts LED table lamp is used along with an Anritsu MS2037C vector analyzer for measuring the antenna S_{11} parameter and pattern measurement as illustrated in Fig. 8. Four different experiments are conducted for measuring the S_{11} parameter of the proposed antenna as shown in Figs 8(d)–8(g). The reverse bias value selected for this antenna measurement is −1V. In Experiment-1, the antenna simulation result shows the radiation at 4.3 GHz and the measurement result shows the radiation at 4.32 GHz. The simulated and measured return losses are −35.4dB and −21 dB respectively. The photodiode switch performance is varied under light with biasing voltage and without DC bias voltage. When DC bias voltage of −0.9 to −1 V is applied to the switches without light(Experiment-2) the photodiode acts as a poor conductor because the value of junction resistance and capacitance

https://doi.org/10.1017/S1759078722000137 Published online by Cambridge University Press

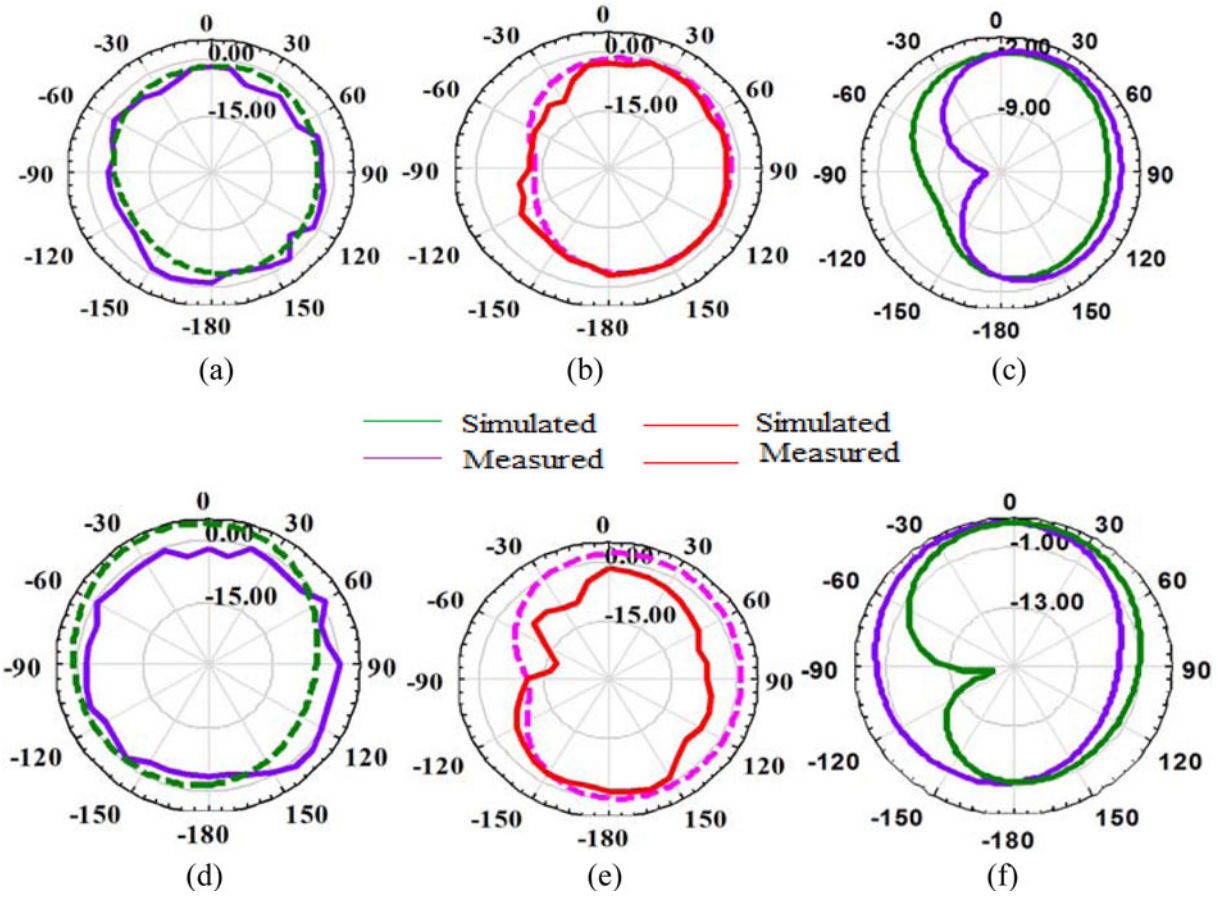


Fig. 10. Radiation pattern of θ_E at(X-Z plane) (a) $\varphi = 0°$ at 4.3 GHz (d) $\varphi = 90°$ at 4.3 GHz (b) $\varphi = 0°$ at 3.5 GHz (e) $\varphi = 90°$ at 3.5 GHz (c) $\varphi = 0°$ at 5 GHz (f) $\varphi = 90°$ at 5 GHz.

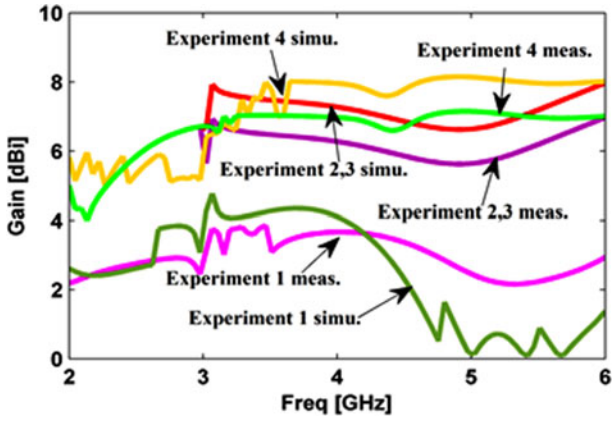


Fig. 11. Gain of the antenna.

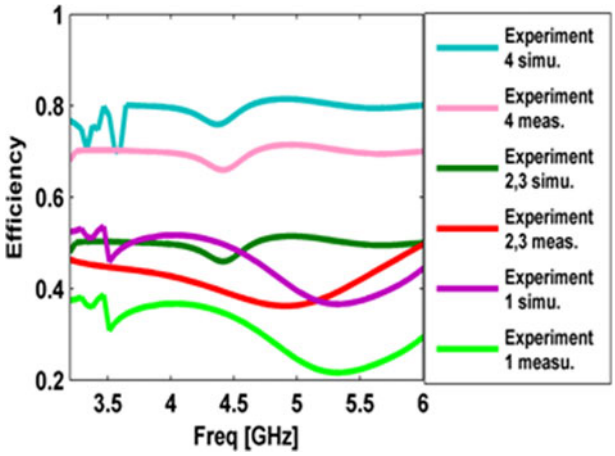


Fig. 12. Efficiency of the antenna.

increases and when the optical signal is applied to the photodiodes without DC bias voltage(Experiment-3) the antenna shifts the radiations at 3.5GHz and 5GHz.The antenna exhibits the radiation at 5 GHz with a return loss value of −20 dB with light and −1V DC bias (Experiment- 4). The simulated and measured return loss values at all experimental conditions are given in Fig. 9 and Table 2.

Figure 10 gives the normalized gain of the antenna at different frequencies (4.3GHz, 3.5GHz, and 5 GHz) under simulation and measured conditions. For the radiation pattern and gain measurement, a standard 12 dB gain horn antenna is used with a 2 m distance from the test antenna. The below comparisons show the accepted normalized gain between the simulation and experiments at $\varphi = 0^o$ and $\varphi = 90^o$. The measured pattern is slightly changed in Experiment −2 and 3 due to losses created from PIN photodiodes, feeder and substrate. These losses are not considered in simulation so the measured gain values are normally lesser than the simulated values.

https://doi.org/10.1017/S1759078722000137 Published online by Cambridge University Press

Figures 11 and 12 shows the efficiency and gain of the antenna. The proposed antenna exhibits maximum gain and efficiency in Experiment-4 and minimum gain and efficiency in Experiment-1. The antenna return loss, gain and efficiency comparisons are given in Table 2.

Conclusion

In this paper, a 47.6% compactness (44 × 28) mm optically controlled frequency reconfigurable antenna prototype is fabricated and their S_{11}, radiation pattern, gain and efficiency parameters are measured experimentally. The fabricated antenna produces frequency reconfiguration from 4.3 to 3.5GHz and 5 GHz with accepted return loss in both measurement and simulation. The designed antenna is a good candidate for future optically controlled IoT devices and wireless applications. The antenna can be used for radio altimeter at 4.3 GHz, WLAN at 5 GHz and 5G applications at 3.5 GHz. The antenna gives a maximum measured gain of 7.2 dBi and 10.2% bandwidth at 5 GHz.

Acknowledgement. This research work was funded by "Visvesvaraya Ph.D Scheme for Electronics & IT" Ministry of Electronics and Information Technology, the Government of India (unique awardees no MEITY-Ph.D-3061).

References

1. **Cui J, Zhang A and Chen X** (2020) Omnidirectional multiband antenna for railway applications. *IEEE Antennas and Wireless Propagation Letters* **19**, 54–58.
2. **Jin G, Deng C, Xu Y, Yang J and Liao S** (2020) Differential frequency-reconfigurable antenna based on dipoles for Sub-6 GHz 5 G and WLAN applications. *IEEE Antennas and Wireless Propagation Letters* **19**, 472–476.
3. **Jose MC, Sankaranjan R, Suseela B, Alsath MGN and Kumar P** (2021) A compact omnidirectional to directional frequency reconfigurable antenna for wireless sensor network applications. *International Journal of Microwave and Wireless Technologies*, 1–12.
4. **Li L, Nan J, Liu J and Tao C** (2021) Compact UWB antenna with triple-band notch reconfigurability. *International Journal of Microwave and Wireless Technologies* **13**, 826–832.
5. **Peng X and Kong L** (2020) Design and optimization of optical receiving antenna based on compound parabolic concentrator for indoor visible light communication. *Optic Communication* **464**, 125447.
6. **Borges RM, Sodré Jr AC and Rodovalho TN** (2015) Reconfigurable multi-band radio - frequency transceiver based on photonics technology for future optical wireless communications. *IET Optoelectronics* **9**, 257–262.
7. **Vian J and Popovic Z** (2000). A transmit/receive active antenna with fast low-power optical switching. *IEEE Transactions on Microwave Theory and Techniques* **48**, 2686–2691.
8. **Pendharker S and Shevgaonkar RK** (2014). Optically controlled frequency-reconfigurable microstrip antenna with low photoconductivity. *IEEE Antennas and Wireless Propagation Letters* **13**, 99–102.
9. **da Costa IF, Spadoti DH, Sodré Jr AC, da Silva LG, Rodriguez S, Puerta R, Olmos JJV and Monroy T** (2017) Optically controlled reconfigurable antenna for 5G future broadband cellular communication networks. *Journal of Microwaves, Optoelectronics and Electromagnetic Applications* **16**, 208–217.
10. **da Costa IF, Arismar Cerqueira Jr S, Spadoti DH, da Silva LG, Ribeiro JAJ and Barbin SE** (2017) Optically controlled reconfigurable antenna array for mm-wave applications. *IEEE Antennas and Wireless Propagation Letters* **16**, 2142–2145.
11. **Konkol MR, Ross DD, Shi S, Harrity CE, Wright AA, Schuetz CA and Prather DW** (2017) High-power photodiode-integrated-connected array antenna. *Journal of Llightwave Technology* **35**, 2010–2016.
12. **Yegnanarayanan S and Jalali B** (2000) Wavelength-selective true time delay for optical control of phased-array antenna. *IEEE Photonics Technology Letters* **12**, 1049–1051.
13. **da Cost IF, Cerqueira A, Reis E, Spadoti DH, Moreira Neto JR, Sapucaí and Indústria R and B** Optically Controlled Reconfigurable Antenna Array Based on a slotted Circular Waveguide. 2015 9th European Conference on Antennas and Propagation - 31 August 2015 ISSN: 2164-3342.
14. **Ullah S, Ullah S, Ahmad I, Khan WUR, Ahmad T, Habib U, Albreem MA, Alsharif MH and Uthansakul P** (2021) Frequency reconfigurable antenna for portable wireless applications. *Computers, Materials & Continua Tech Science Press* **68**, 3015–3027. doi: 10.32604/cmc.2021.015549.
15. **Zhang Y, Lin S, Yu S, Liu GJ and Denisov A** (2018) Design and analysis of optically controlled pattern reconfigurable planar Yagi–Uda antenna. *IET Microwaves, Antennas & Propagation* **12**, 2053–2059. doi: 10.1049/iet-map.2018.5204.
16. **Xu B, Liu Z and Yue CP** (2020) An Ac-Powered smart LED Bulb for 3D Indoor Localization Using VLC, *2019 IEEE 8th Global Conference on Consumer Electronics(GCCE)*, Feb-2020, ISSN:2378-8143.
17. **Zhao D, Lan L, Han Y, Liang F, Zhang Q and Wang B-Z** (2014) Optically controlled reconfigurable band-notched UWB antenna for cognitive radio applications. *IEEE Photonics Technology Letters* **26**, 2173–2176.
18. **Panagamuwa CJ and Chauraya A** (2006) Frequency and beam reconfigurable antenna using photoconducting switches. *IEEE Transactions on Antennas and Propagation* **54**, 449–454.
19. **Patron D, Daryoush AS and Dandekar KR** (2014) Optical control of reconfigurable antennas and application to a novel pattern-reconfigurable planar design. *Journal of Light Wave Technology* **32**, 3394–3402.
20. **Reji V and Manimegalai CT** (2021) V-shaped long wire frequency reconfigurable antenna for WLAN and ISM band applications. *International Journal of Electronics and Communications* **140**, 153937.



V. Reji received the bachelor of engineering degree in electronics and communication engineering from Manonmanium Sundaranar University, Tamilnadu, India, in 2003. She received the master of engineering degree in communication systems from SRM University, India in 2011. Currently, She is doing her research in SRM Institute of Science and Technology, Chennai, India under "Visvesvaraya Ph.D Scheme for Electronics & IT" Ministry of Electronics and Information Technology, India.



Dr. C. T. Manimegalai is currently working as an associate professor in the Department of ECE, SRM Institute of Science and Technology, Chennai, India. She has done her Ph.D in wireless communication in the year 2014. Her area of specialization includes wireless communication, antenna design and optical communication. She has received various funds from the government of India and filed patents. She is a member of several professional societies and a reviewer of reputed journals. She has published several papers in refereed journals.

https://doi.org/10.1017/S1759078722000137 Published online by Cambridge University Press